Acta Biomaterialia 9 (2013) 7289–7297

Contents lists available at SciVerse ScienceDirect

Acta Biomaterialia

journal homepage: www.elsevier.com/locate/actabiomat

An amelogenin–chitosan matrix promotes assembly of an enamel-like layer with a dense interface

Qichao Ruan [a], Yuzheng Zhang [b], Xiudong Yang [a], Steven Nutt [b], Janet Moradian-Oldak [a,*]

[a] Center for Craniofacial Molecular Biology, Herman Ostrow School of Dentistry, University of Southern California, Los Angeles, CA 90033, USA
[b] Mork Family Department of Chemical Engineering and Materials Science, University of Southern California, Los Angeles, CA 90089, USA

ARTICLE INFO

Article history:
Received 18 January 2013
Received in revised form 4 March 2013
Accepted 1 April 2013
Available online 6 April 2013

Keywords:
Enamel
Amelogenin
Chitosan hydrogel
Apatite
Biomimetic

ABSTRACT

Biomimetic reconstruction of tooth enamel is a significant topic of study in materials science and dentistry as a novel approach to the prevention, restoration, and treatment of defective enamel. We have developed a new amelogenin-containing chitosan hydrogel for enamel reconstruction that works through amelogenin supramolecular assembly, stabilizing Ca-P clusters and guiding their arrangement into linear chains. These amelogenin Ca-P composite chains further fuse with enamel crystals and eventually evolve into enamel-like co-aligned crystals, anchored to the natural enamel substrate through a cluster growth process. A dense interface between the newly grown layer and natural enamel was formed and the enamel-like layer improved the hardness and elastic modulus compared with etched enamel. We anticipate that this chitosan hydrogel will provide effective protection against secondary caries because of its pH-responsive and antimicrobial properties. Our studies introduce an amelogenin-containing chitosan hydrogel as a promising biomaterial for enamel repair and demonstrate the potential of applying protein-directed assembly to biomimetic reconstruction of complex biomaterials.

1. Introduction

Enamel is the exterior layer of the mammalian tooth and a hard biomaterial with significant resilience that protects the tooth from external physical and chemical damage [1]. The remarkable mechanical properties of enamel are associated with its hierarchical levels of structure from the nanoscale to the macroscale [2]. The building blocks of enamel, the enamel rods, are densely packed arrays of elongated apatite crystals organized into an intricate interwoven structure [2]. Cellular activity and the protein-controlled process of mineralization are key to achieving such precisely organized structures [1]. The proteins that mediate the mineralization of apatite crystals are gradually degraded and eventually removed during enamel maturation [1,3,4]. Mature enamel is non-living and cannot regenerate itself after substantial mineral loss, which often occurs as dental caries or erosion. Currently the conventional treatments for carious lesions include refilling with amorphous materials like amalgam, ceramics, or composite resin [5]. However, even after those treatments secondary caries often arises at the interface between the original enamel and the filling materials due to weakening adhesion over time [6]. There is therefore a need for alternative restorative materials with improved adhesion to the tooth surface. One such alternative is a synthetic enamel-like material that can be prepared by biomimetic regrowth on the enamel surface.

Various biomimetic systems have been developed to repair enamel defects, including liquids and pastes that contain nano-apatite or different organic additives, for the remineralization of early, sub-micrometer sized enamel lesions. A glycerine-enriched gelatin system has been used to form dense fluorapatite layers on human enamel [7,8]. Growth in small cavities of enamel-like nanocrystals from a paste containing fluoride-substituted hydroxyapatite has been achieved in vitro [9], and a compacted fluorapatite film with a prism-like structure was synthesized on metal plates using a hydrothermal technique [10]. Formation of enamel-like structures under ambient conditions was also performed in vitro using a liquid and pastes with different organic additives [11–15]. Recently an electrospun hydrogel mat of amorphous calcium phosphate (ACP)/poly(vinylpyrrolidone) nanofibers was developed for the in vitro remineralization of dental enamel [16]. These investigations constitute significant progress in the study of enamel-like structures. Overall, however, biomimetic strategies still face an ongoing challenge in the fields of dentistry and material science.

In natural enamel the formation of apatite crystals occurs in an amelogenin-rich matrix that plays a critical role in controlling the oriented and elongated growth of apatite crystals [4,17–20]. Accordingly, we have used several strategies to prepare enamel-like materials that contain nano- and microstructures using amelogenin to control the crystallization of biomimetic

* Corresponding author. Tel.: +1 323 442 1759; fax: +1 323 442 2981.
E-mail address: joldak@usc.edu (J. Moradian-Oldak).

1742-7061/$ - see front matter © 2013 Acta Materialia Inc. Published by Elsevier Ltd. All rights reserved.
http://dx.doi.org/10.1016/j.actbio.2013.04.004

calcium and phosphate [20–23]. The results have opened up the promising possibility of remodeling complex enamel minerals in an amelogenin-containing system.

Here we report development of a new amelogenin-containing chitosan (CS-AMEL) hydrogel to synthesize an organized, enamel-like mineralized layer on an acid-etched enamel surface used as an early caries model. Compared with a previously developed amelogenin-containing system, CS-AMEL is easier to handle under clinical conditions. It is biocompatible, biodegradable, and has unique antimicrobial and adhesion properties that are practical for dental applications [24–26]. Chitosan has been observed to have antimicrobial activity against fungi, viruses, and some bacteria, including streptococci and lactobacilli, which are known as the principal etiological factors of dental caries [27–29]. Therefore, we expect that the "synthetic enamel" formed in the CS-AMEL hydrogel will have antimicrobial properties that can prevent bacterial infection and subsequent demineralization. In addition, chitosan is mucoadhesive to both hard and soft surfaces [30]. Importantly, the newly formed crystals in the CS-AMEL hydrogel grow directly on the original enamel, achieving complete adhesion of the repaired layer to the natural enamel with a dense interface. The robust attachment of the newly grown layer demonstrated in the present work can potentially improve the durability of restorations and avoid the formation of new caries at the margin of the restoration.

2. Materials and methods

2.1. Amelogenin preparation

Recombinant full-length porcine amelogenin rP172 was expressed in *Escherichia coli* and purified as previously described. The rP172 protein has 172 amino acids and is an analog of full-length native porcine P173, but lacking the N-terminal methionine as well as a phosphate group on Ser16 [20–23].

2.2. Tooth slice preparation

Human third molars (extracted following the standard procedures for extraction at the Ostrow School of Dentistry of the University of Southern California and handled with the approval of the Institutional Review Board) without any restored caries were selected. Slices 0.1–0.2 cm thick (Fig. 1a) were cut longitudinally using a water-cooled low speed diamond saw. To simulate early caries lesions tooth slices were acid etched with 30% phosphoric acid for 30 s and rinsed with deionized water.

2.3. Etched enamel repaired by the amelogenin-containing chitosan hydrogel

The amelogenin-containing chitosan hydrogel was prepared by mixing chitosan (medium molecular weight, 75–85% deacetylated, Sigma–Aldrich) solution (960 μl, 1% m/v), Na_2HPO_4 (15 μl, 0.1 M), $CaCl_2$ (25 μl, 0.1 M) and amelogenin rP172 (200 μg), followed by stirring at room temperature overnight. The pH value was adjusted to 6.5 with 1 M NaOH. 20 μl of chitosan-based hydrogel was carefully applied to the enamel surface and dried in air at room temperature. The tooth slices were then immersed in 30 ml of artificial saliva (AS) solution (0.2 mM $MgCl_2$, 1 mM $CaCl_2{\cdot}H_2O$, 20 mM HEPES buffer, 4 mM KH_2PO_4, 16 mM KCl, 4.5 mM NH_4Cl, 300 p.p.m. NaF, pH 7.0, adjusted with 1 M NaOH) [16] at 37 °C for 7 days. After the allotted time the tooth slice was removed from the solution, rinsed with running deionized water for 50 s and air dried.

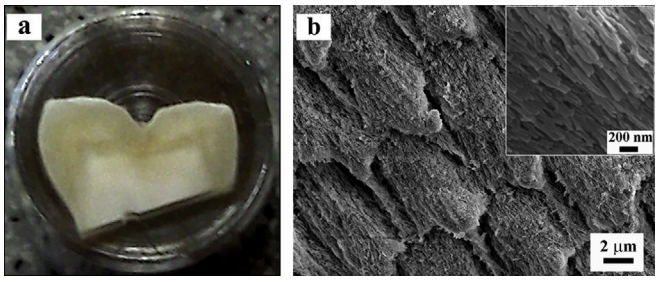

Fig. 1. (a) Optical micrograph of a tooth slice used in this work. (b) SEM image of an acid etched enamel surface.

2.4. Characterization

Scanning electron microscopy (SEM) imaging was performed in a field emission scanning electron microscope (JEOL JSM-7001F), operating at an accelerating voltage of 10 keV. X-ray diffraction (XRD) patterns were recorded in a Rigaku diffractometer with Cu K_α radiation (λ = 1.542 Å) operating at 70 kV and 50 mA with a step size of 0.02°, at a scanning rate of 0.1°s^{-1} in the 2θ range 10–60°. Thin sections (~100 nm) between enamel and the newly grown layer for the TEM observations were prepared in a SEM/FIB (JEOL JIB-4500) with an ion accelerating voltage of 30 kV. The device was also equipped with an in situ lift-out system (Omniprobe Autoprobe 200), which had a tungsten needle attached to a micromanipulator inside the FIB vacuum chamber. High resolution transmission electron microscopy (HR-TEM) images were obtained on a JEOL JEM-2100 microscope using an accelerating voltage of 200 keV. The hardness and elastic modulus were measured at 20 test points in each sample (n = 3) using a nano-indenter (Agilent-MTS XP) with a Berkovich tip. Circular dichroism (CD) spectropolarimetry was performed using a J-815 spectropolarimeter (JASCO, Easton, MD). The spectra were recorded between 190 and 260 nm with a step size of 0.5 nm and a scan rate of 50 nm min^{-1}. Fluorescence spectroscopy was performed using a PTI QuantaMaster QM-4SE spectrofluorometer (PTI, Birmingham, NJ). The amelogenin solutions were excited at 290 nm. The emission spectra were monitored between 300 and 400 nm with a step size of 1 nm.

2.5. Antimicrobial evaluation

Human saliva was collected as described in the literature [31] for the antimicrobial experimentation. Healthy adults were chosen as the subjects for saliva collection. Subjects were asked to refrain from eating, drinking, and oral hygiene procedures for at least 1 h prior to collection. Subjects were given distilled drinking water and asked to rinse their mouths out with it for 1 min. Five min after this oral rinse the subjects were asked to spit into a 50 ml sterile tube, which was placed on ice while more saliva was collected. The subjects were instructed to tilt their head forward and let the saliva run naturally to the front of the mouth; Upon collection of approximately 5 ml of saliva from a subject the saliva sample was immediately taken to the laboratory for processing. Twenty μl of saliva were added to tubes with 1 ml of lysogeny broth (LB) medium containing chitosan–amelogenin hydrogel or amelogenin, and then incubated at 37 °C overnight. The OD_{600} of the overnight cultures was measured using a Beckman DU-640 spectrophotometer.

2.6. Statistical analysis

Enamel remineralization experiments were repeated three times. The mechanical tests and antimicrobial experiments were conducted in triplicate and data were expressed as means ± standard deviations. For mechanical testing Student's t-test was applied to identify differences in the hardness and elastic modulus between etched and repaired enamel (n = 3). For the antimicrobial experiments (n = 3) the OD values were compared between control and

samples containing chitosan–amelogenin hydrogel or amelogenin by the same test. In all experiments the differences were considered statistically significant at $P \leqslant 0.05$ and highly significant at $P < 0.001$. All the statistical analyses were carried out using Origin 8.0 (Origin Lab, Northampton, MA) and Microsoft Office Excel 2007.

3. Results and discussion

3.1. Enamel remineralization without CS-AMEL hydrogel

Dental caries is caused by an imbalance in the dynamic process of demineralization–remineralization of enamel [32]. Enamel demineralization occurs at low pH caused by acids of bacterial origin. To produce artificial caries a tooth slice was etched with 30% phosphoric acid. When examined the etched enamel crystals were seen to be discontinuous and broken, resembling crystals from carious enamel (Fig. 1b) [33]. Although the calcium and phosphate ions in the saliva permit recovery of some lost enamel mineral, the remarkably organized structure of enamel cannot be regained without protein mediation. We prepared an AS solution to simulate the oral environment for enamel remineralization. After soaking in AS solution alone for 7 days a calcium phosphate coating with a thickness of 1 μm had formed on the surface of enamel. As shown in Fig. 2a and b, the remineralized crystals had a rod-like structure and the coating was porous. A similar layer but with a thickness of 10 μm formed on the etched enamel soaked in chitosan hydrogel without amelogenin. This remineralized apatite layer also consisted of loosely packed crystals with a porous structure (Fig. 2c and d). These porous layers did not resemble natural enamel structure, which has a high packing density of apatite crystals.

3.2. Enamel remineralization with CS-AMEL hydrogel

Fig. 3 shows the microstructures of human molar enamel and the newly grown layer on an etched enamel surface soaked for 7 days in CS-AMEL hydrogel. At the nanoscale (Fig. 3a) natural enamel is made of highly organized arrays of apatite crystallites growing preferentially along the *c*-axis, perpendicular to the surface (black arrows in Fig. 3a). After mineralization for 7 days similar organized crystals were formed on the etched enamel surface treated with CS-AMEL hydrogel. The crystals grown in CS-AMEL hydrogel were composed of numerous nanorods oriented preferentially along the *c*-axis with a diameter of ~50 nm, nearly parallel to each other in the longitudinal direction (white arrows in Fig. 3b). The newly grown layer, with a thickness of 15 μm, was tightly bound to the surface of the natural enamel (Fig. 3b, inset). Examination at higher magnification revealed no obvious boundary at the interface (Fig. 3c). The bulk of the newly grown layer contained needle-like crystals that were bundled to form a fundamental organization unit analogous to that of natural enamel crystallites (Fig. 3d and e). The HR-TEM image showed clear lattice fringes perpendicular to the nanorod axis with an interplanar spacing of $d = 0.3429$ nm, in accordance with the distance between the (002) crystal planes of hydroxyapatite (JCPDS 09-0432), which suggests that the nanorods formed in CS-AMEL hydrogel grow in the [001] direction (white arrow in Fig. 3e). Selected area electron diffraction (SAED) of the newly grown layer resulted in an arc-shaped pattern along the (002) diffraction plane, indicating a hierarchical alignment of the *c*-axes of the newly formed crystals (Fig. 3f).

The orientation and composition of the newly grown crystals were further confirmed by X-ray diffraction (XRD) and energy dispersion spectroscopy (EDS) (Fig. 4). All of the diffraction peaks can be readily indexed to hexagonal phase hydroxyapatite (JCPDS 09–0432) crystals. The unsplit diffraction peak around $2\theta = 32^\circ$ indicates the poor crystallinity of newly formed apatite in the CS-AMEL hydrogel (Fig. 4a) [34]. Sharp and intense 002 and 004 peaks indicate that the (001) faces are parallel to the surface (Fig. 4a), i.e. the crystals align in an orderly fashion along the crystallographic *c*-axis, in accordance with the microstructure seen by SEM and TEM observation (Fig. 3). EDS revealed the presence of calcium, phosphate and fluorine ions in the newly grown layer (Fig 4b). The structural and compositional analyses indicated that the newly formed layer contain fluoridated hydroxyapatite with poor crystallinity [17].

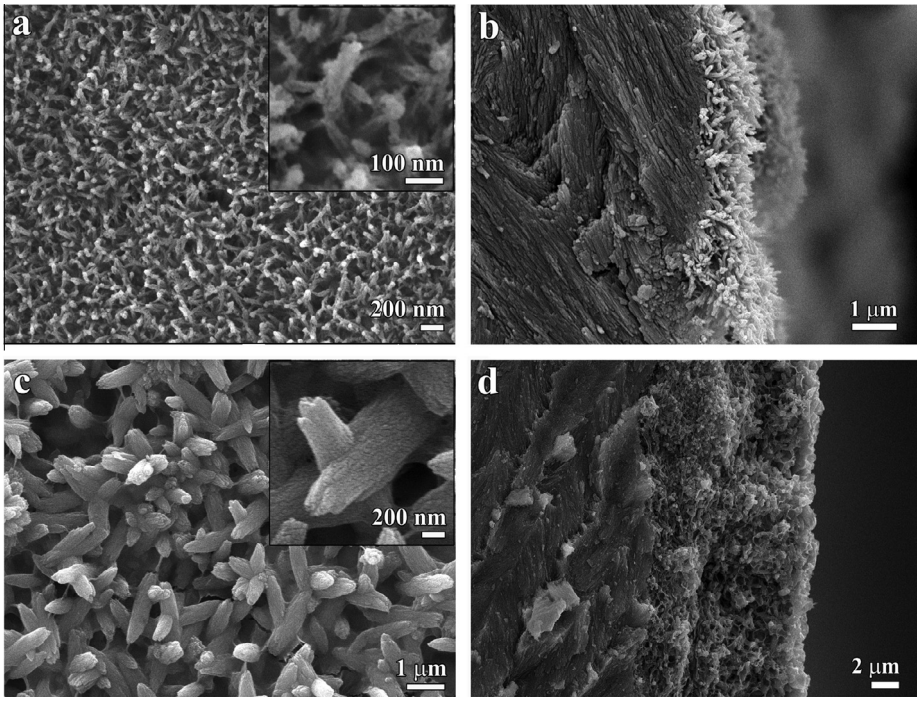

Fig. 2. SEM images of the newly grown layer without amelogenin after remineralization in an artificial saliva solution for 7 days. (a, c) Top view; (b, d) side view. (a, b) Without chitosan gel; (c, d) with chitosan gel.

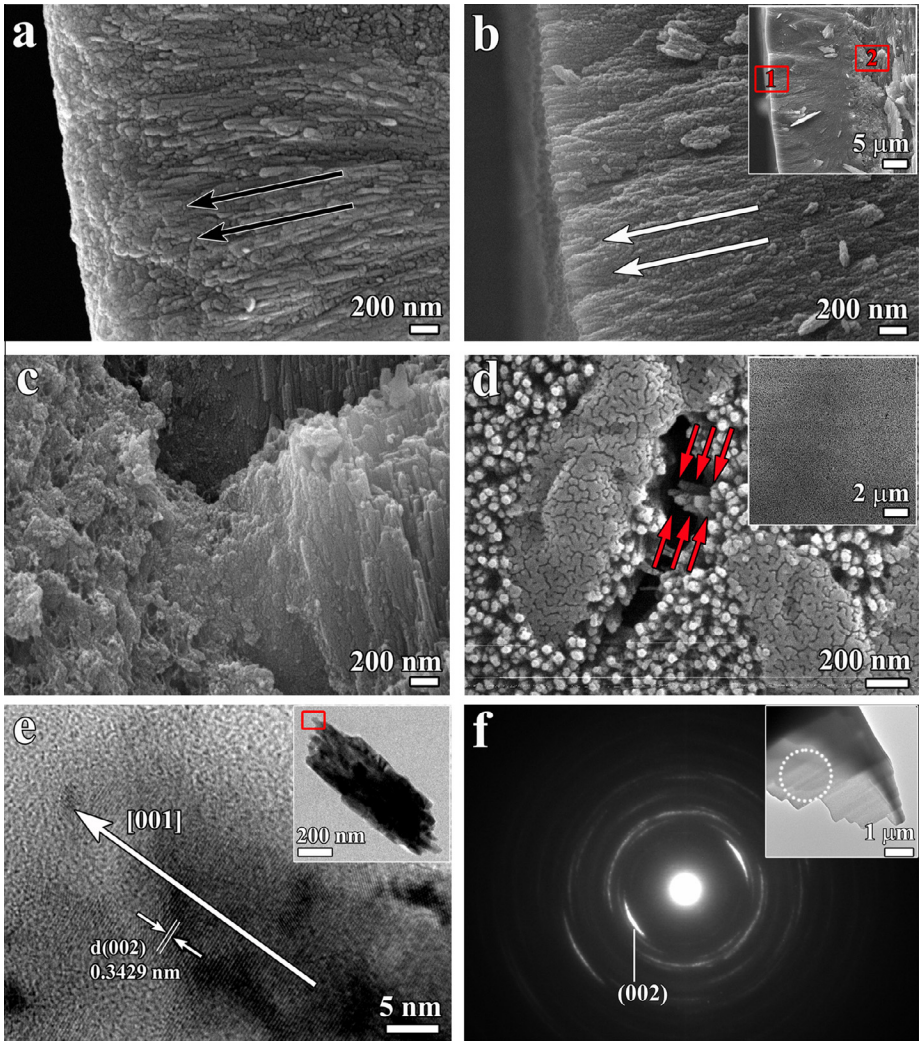

Fig. 3. SEM and TEM images of natural enamel and the newly grown layer after remineralization in amelogenin–chitosan gel for 7 days. (a) Microstructure of native enamel. Black arrows indicate the crystallographic orientations of the apatite crystallites in native enamel. (b) After 7 days remineralization with chitosan–amelogenin hydrogel an enamel-like layer had formed on the surface of etched enamel. (Inset) Thickness of the newly grown layer. Rectangles 1 and 2 represent the selected areas corresponding to (b) and (c). White arrows indicate the apatite orientations in the newly grown layer. (c) The newly grown layer was firmly bound to the surface of the enamel. (d) Bundles of organized crystals were found inside the repaired layer. The arrows indicate a typical bundle of parallel crystals inside the newly grown layer. (Inset) The homogeneous surface of the repaired layer. (e) HR-TEM image of a rod-like crystal taken from the area outlined by the red rectangle on the crystal bundle in the inset. The arrow indicates the crystallographic direction of an apatite crystal along the *c*-axis. The HR-TEM image represents a typical bundle of parallel crystals. (f) SAED image of the newly grown layer. (Inset) TEM image of the repaired layer prepared by focused ion beam (FIB) milling.

3.3. Functions of chitosan and amelogenin in enamel remineralization with CS-AMEL hydrogel

Comparing the morphologies of the remineralized layers formed in the chitosan hydrogel with and without amelogenin, we observed that disordered structures with a porous morphology were formed without the protein (Fig. 2), but ordered enamel-like structures were obtained in the presence of amelogenin (Fig. 3b–f). These results indicate that amelogenin mediation is an essential factor for the formation of orderly enamel-like structure in the chitosan hydrogel system. Although chitosan hydrogels has also been reported as a mineralization matrix because of its charged surface [35], chitosan molecules were not found to affect the function of amelogenin during synthesis of the repaired layer.

The chitosan–amelogenin interaction was studied using CD and fluorescence spectroscopy at pH 3.5, 5.5 and 8.0 (Fig. 5). All the CD spectra of pure amelogenin showed negative ellipticities around 203 nm, which are characteristic of unordered polyproline type II structures [36]. At pH 3.5 the intensity of the minima gradually increased and the trough shifted to a higher wavelength with increasing ratios of chitosan to amelogenin, indicating a possible change in the conformation of amelogenin in the presence of chitosan. In the corresponding fluorescence spectra red shifts of the emission maxima were also observed with increasing amounts of chitosan, indicating the exposure of tryptophan residues in amelogenin (Fig. 5a) [37,38]. These changes in the CD and fluorescence spectra clearly illustrated that there was a direct interaction between amelogenin and chitosan at pH 3.5. At pH 5.5 both the intensity of the negative dichroic signals and the positions of their minima were changed on the addition of chitosan to amelogenin, however, there was no shift in the fluorescence spectra (Fig. 5b). When the pH reached 8.0 it was difficult to find the dichroic signal or the emission band in the CD and fluorescence spectra of amelogenin in association with chitosan (Fig. 5c). The results from the CD and fluorescence spectra revealed that the interaction between chitosan and amelogenin is dependent on pH. At pH values below the pK_a of chitosan (6.5) [39] the amino groups were almost completely ionized, and the charge density of chitosan increased;

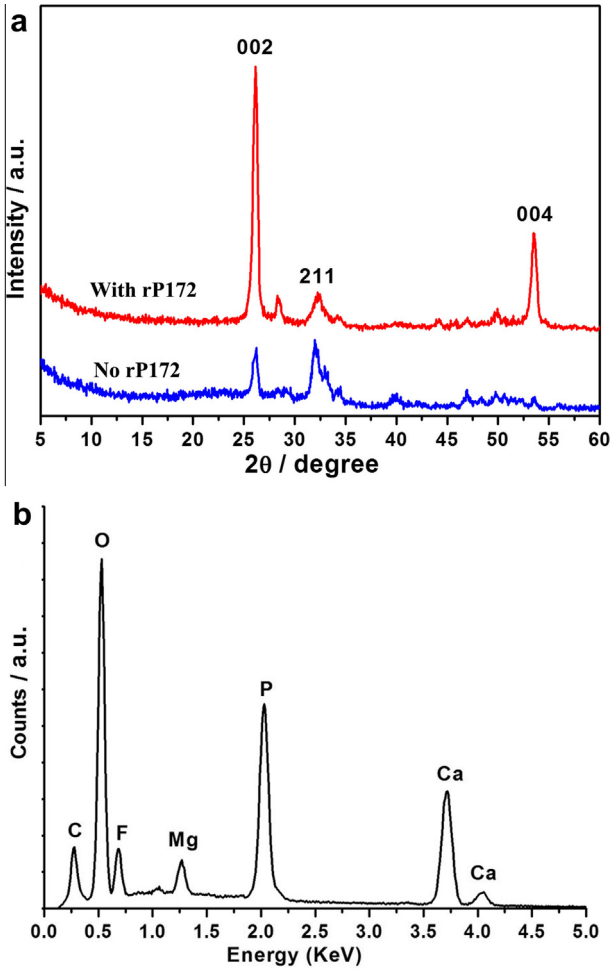

Fig. 4. (a) XRD spectra of the newly grown layer after remineralization in a chitosan gel with and without amelogenin for 7 days. (b) EDS spectrum of the repaired layer after remineralization in a chitosan gel with amelogenin for 7 days.

thus chitosan interacted with amelogenin through electrostatic interaction. In contrast, when the pH was higher than 5.5 the interaction with chitosan was weak because of its low solubility and deprotonation.

Therefore, under our experimental conditions (pH > 6.5) amelogenin is the crucial factor in controlling the oriented growth of fluoridated hydroxyapatite crystals. Even so, the role of chitosan is likely more than just as an amelogenin carrier. Chitosan in the CS-AMEL system could provide effective protection from enamel erosion because of its pH responsiveness. The development of caries is associated with a continuous pH change in the plaque biofilm due to the accumulation of acid by-products from metabolism of fermentable carbohydrates [32,40,41]. As the pH decreases (in the general range 5.5–5.0) positive hydrogen ions from the acids bind to the negative phosphate and hydroxyl ions from enamel mineral, leading to mineral loss. The potential advantage of having chitosan present on the enamel surface is that the amino groups of chitosan could capture the acid hydrogen ions, forming a positive protective layer preventing the diffusion of hydrogen ions to the mineral surface, as well as interacting with amelogenin to avoiding amelogenin loss into the saliva. When the normal pH is restored (to the range 6.3–7.0) by saliva [42] the weakly interacting amelogenin would be released from the chitosan to regulate the remineralization of enamel.

Our HR-TEM and SEM analyses provide further insight into the function of amelogenin in the remineralization of newly grown mineral. In the original CS-AMEL hydrogel we observed linear chains of ~10 nm nanoclusters, as shown in Fig 6a. The calcium phosphate (Ca-P) clusters formed under Ca-P supersaturated conditions are thought to be the building blocks of both amorphous Ca-P as well as the apatitic mineral phase [43,44]. Generally, without a stabilizing agent these Ca-P clusters aggregate randomly to form plate-like mineral particles [45,46]. Indeed, we could not find any oriented aggregation of Ca-P clusters in the original chitosan hydrogel in the absence of amelogenin. We suggest that the presence of amelogenin provides an opportunity for stabilization of the precritical clusters at a minimum free energy, since the co-assembly of amelogenin–Ca-P clusters imparts kinetic and thermodynamic stability to the system [46]. As a result, and as in previous studies [45,46], we suggest that amelogenin assemblies stabilized the Ca-P clusters in the CS-AMEL hydrogel and guided arrangement of the clusters into linear chains that eventually evolved into enamel-like co-aligned crystals anchored to the natural enamel substrate.

3.4. Continuous growth of newly formed crystals on the enamel

SEM images of the side view of a layer grown in CS-AMEL hydrogel for 3 days (Fig. 6b) indicate that the newly grown crystals are mostly oriented perpendicular to the surface of the substrate and in non-prismatic orientations (white arrows in Fig. 6b). The interface between the repaired layer and the enamel substrate, indicated by the dotted line, reveals no apparent gap. To further explore the interface microstructure we used a focused ion beam (FIB) technique to prepare TEM samples for higher resolution analysis. Fig. 6c depicts a HR-TEM image of the interface where the new crystals nucleate, clearly exhibiting lattice fringes from the (3 0 1) and ($1\,0\,\bar{3}$) planes of the enamel crystal (d = 0.261 nm and d = 0.236 nm), as well as the (0 0 2) plane of the synthetic crystal (d = 0.339). The corresponding fast Fourier transform (FFT) images (inset in Fig. 6c) show two different patterns, indicating that the crystals in the enamel and in the fused repaired layer grew with different orientations, which is consistent with the SEM observations in Fig. 6b. Remarkably, the enamel and the newly grown crystals fused together to form a seamless interface (black arrows in Fig. 6c).

Although the exact growth mechanism remains unresolved, it is clear that amelogenin-stabilized clusters with orientated aggregation are crucial to the continuous growth of new crystals on the enamel. Recent research has shown that calcium-based biominerals can be formed at a templating surface via stable pre-nucleation clusters, with aggregation into an amorphous precursor phase and transformation of this phase into a crystal [47,48]. Similarly to these cluster growth models [48,49], the newly grown crystals formed in CS-AMEL hydrogel in our experiments started with the aggregation of pre-nucleation clusters leading to the nucleation of amelogenin–Ca-P and then the development of oriented apatite crystals. The possible repair processes are schematically presented in Fig. 6d. Initially the pre-nucleation Ca-P clusters, stabilized by amelogenin, aggregate to form linear chains in the CS-AMEL hydrogel. Subsequently parts of the cluster aggregates in contact with the enamel surface become dense by adopting a closer packing of the clusters. The continuation of this process leads to the formation of an amorphous precursor phase that further fuses with enamel crystals and ultimately transforms into crystalline apatite, which is oriented along the c-axis as directed by amelogenin. As a result the newly formed crystals continuously grow on the enamel crystals and are oriented by amelogenin so that their long axes run perpendicular to the enamel surface, like natural enamel prisms [2].

3.5. Bonding strength between the newly grown layer and enamel surface

The dense interface between the synthetic and natural enamel crystals promoted strong bonding between the newly grown layer

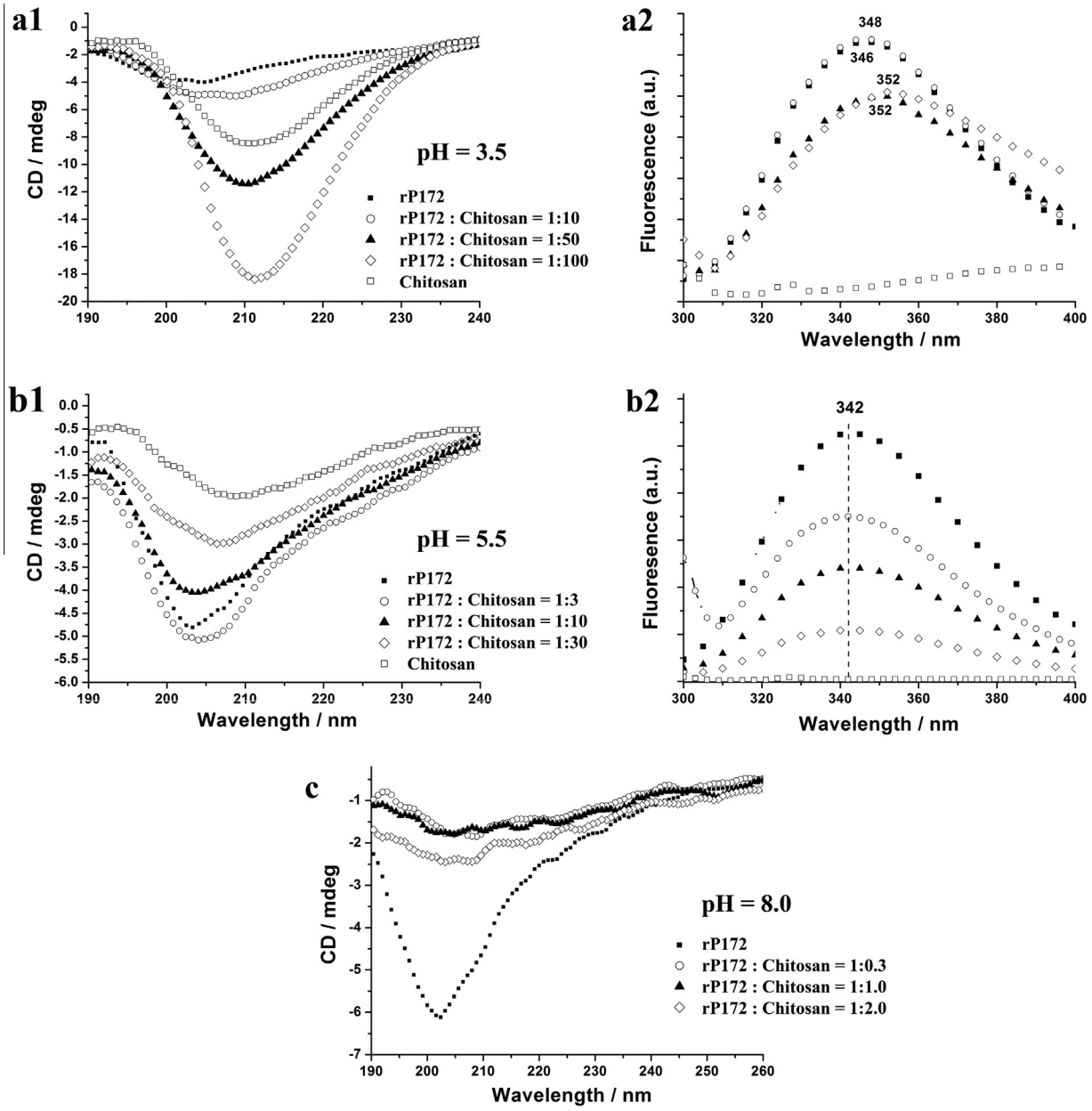

Fig. 5. CD and fluorescence spectra measured at different mass ratios at pH (a) 3.5, (b) 5.5 and (c) 8.0, revealing that the interaction between chitosan and amelogenin is pH dependent.

and the tooth surface. Fig. 7 shows backscattered electron and secondary electron images of the newly grown layer after ultrasonic treatment (42 kHz, 100 W) for 10 min. The results revealed that the newly grown layer formed in the CS-AMEL hydrogel was tightly bound to the enamel surface (Fig. 7a), and the organized structure was unaffected by ultrasonic treatment (Fig. 7b). In contrast, following the same treatment we observed a large gap between the enamel and the repaired layer formed in a chitosan hydrogel without amelogenin (Fig. 7c). In clinical dentistry bonding strength is one of the most important attributes for enamel restorative materials. Due to poor adhesion leading to gaps at the enamel–restoration interface the currently available materials often have limitations in terms of their durability. These gaps increase the possibility for bacterial leakage and secondary caries, which are the main causes of restoration failure [49]. In the present study robust attachment of the newly grown layer formed in the CS-AMEL hydrogel can potentially improve the durability of restorations and avoid the formation of new caries at the margin of the restoration.

3.6. Mechanical properties of the reconstructed enamel-like layer repaired by CS-AMEL hydrogel

Fig. 8a shows the hardnesses and elastic modulus of healthy enamel, etched enamel, and the reconstructed enamel-like layer repaired by a chitosan hydrogel with and without amelogenin. The hardness and modulus of a caries-free enamel slice were estimated to be 4.0 and 70 Gpa, respectively [50], and both the hardness and modulus were severely compromised by acid etching (nearly 88% decrease in modulus and 98% decrease in hardness). After mineralization in a chitosan hydrogel without amelogenin we observed only slight increase in the hardness and modulus of the etched enamel surface (Fig. 8a). Clearly the porous structure (Fig. 2c and d) caused by conventional remineralization could not provide

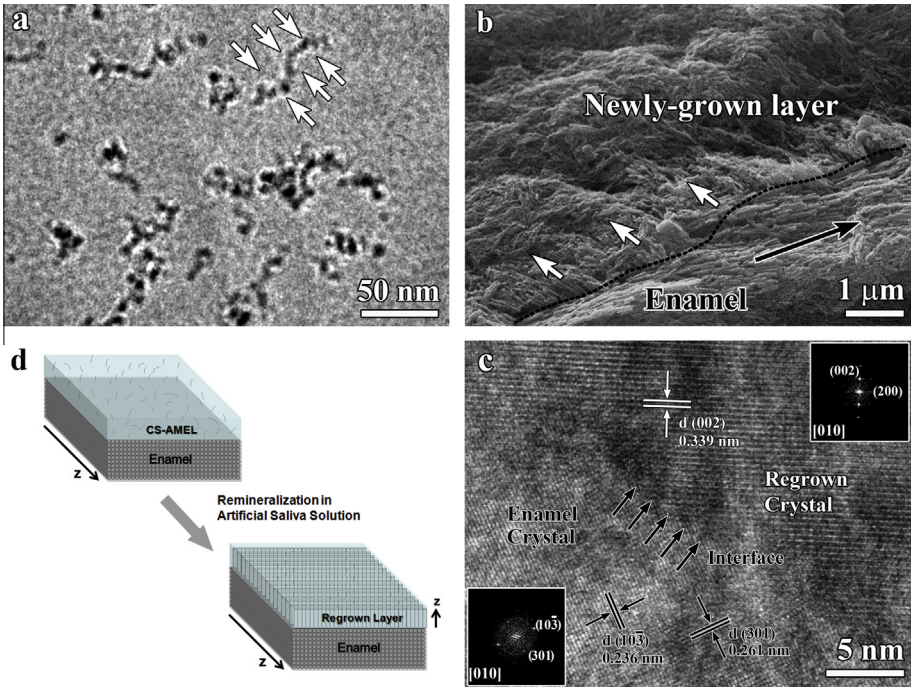

Fig. 6. (a) TEM image of the original CS-AMEL hydrogel showing the elongated nanochain-like structure (white arrows). (b) Cross-section SEM image of the repaired layer after remineralization in amelogenin–chitosan gel for 3 days fused to the surface of the natural enamel. The white and black arrows indicate the crystallographic orientations of the crystals in the newly grown layer and natural enamel, respectively. The dotted line shows the boundary of the natural enamel and the newly grown layer. (c) HR-TEM image of the interface between the enamel and regrown crystal, showing seamless growth of the repaired crystal on the enamel. The black arrows indicate the interface between regrown and enamel crystals. (Inset) FFT images corresponding to enamel and regrown crystals. (d) Schematic illustration of the enamel repair process.

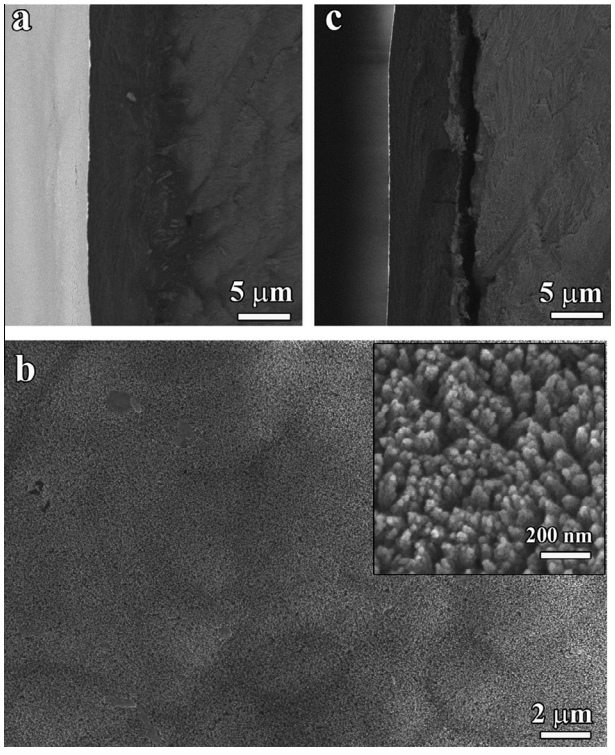

Fig. 7. SEM images of reconstructed enamel-like layers after ultrasonic treatment. (a) Backscattered electron image of a cross-section and (b) second electron image of the surface of an ultrasonically treated newly grown layer obtained in chitosan–amelogenin hydrogel. (Inset) The typical morphology of the surface at higher magnification. (c) Backscattered electron image of a cross-section of an ultrasonically treated newly grown layer obtained in chitosan hydrogel without amelogenin.

satisfactory mechanical functions. However, after treatment with amelogenin-chitosan hydrogel for 7 days the hardness and modulus of the etched enamel surface increased significantly ($P < 0.001$). The modulus increased by nearly four times and the hardness was increased by nearly nine times (Fig. 8a). Although the mechanical properties were not the same as those of native enamel, the repaired enamel treated with CS-AMEL hydrogel showed superior properties compared with the control (without amelogenin) due to the well-organized crystal orientation [51]. The amelogenin and chitosan residues in the repaired layer may limit its mechanical performance, which could potentially be improved by removal of the organic material using proteolytic enzymes [52–54]. Moreover, in clinical practice the mechanical properties of the repaired layer could be further improved by repetitive application of CS-AMEL hydrogel in order to achieve a thicker repaired layer. Further work is needed in order to assess the stability of the CS-AMEL hydrogel in the oral cavity.

3.7. Antimicrobial properties of the CS-AMEL hydrogel

Human saliva used as a source of bacteria was cultured in LB medium to examine the antimicrobial properties of CS-AMEL by observing the optical density (OD) values and turbidity (Fig. 8b). After overnight culture the medium without chitosan gel was opaque due to presence of bacteria, while the medium with chitosan gel was clear (inset in Fig. 8b). The OD value was significantly reduced when CS-AMEL hydrogel was added to the LB medium ($P < 0.001$, Fig. 8b). These results demonstrate that the CS-AMEL hydrogel can effectively inhibit bacterial growth. We believe that the antimicrobial effect of the CS-AMEL hydrogel was attributable to chitosan. Chitosan has been observed to have antimicrobial activity against a wide variety of bacteria, including streptococci and lactobacilli, which are known as the principal etiological factors in dental caries. Moreover, chitosan has several advantages

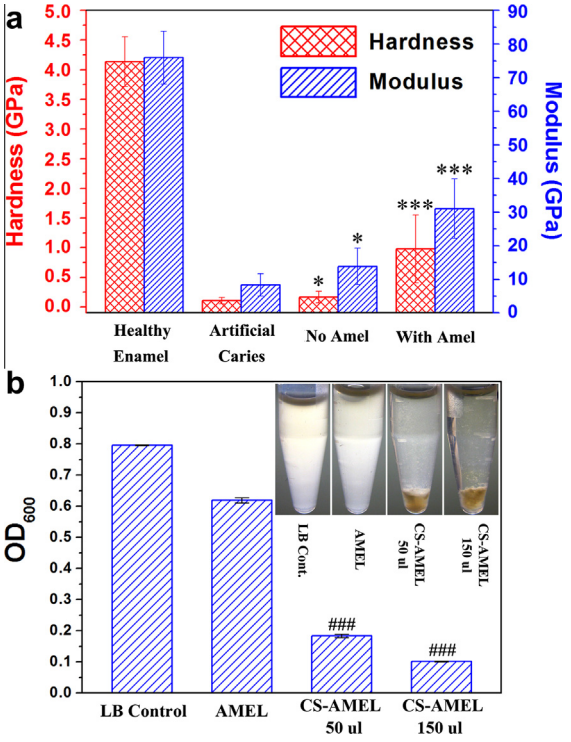

Fig. 8. (a) Hardness and elastic modulus of healthy enamel, etched enamel, and reconstructed enamel repaired by chitosan hydrogel with and without amelogenin. $^{*}P \leqslant 0.05$ compared with artificial caries; *** $P < 0.001$ compared with artificial caries. (b) OD values of the overnight cultures of saliva bacteria in different LB media. $^{\#\#\#}P < 0.001$ compared with LB control. (Inset) Turbidity of the LB medium with and without chitosan hydrogel.

over other types of antiseptic agents, including a higher antibacterial activity, a broader spectrum of activity, a higher killing rate, and lower toxicity to mammalian cells [55]. Therefore, we expect that clinical application of the CS-AMEL hydrogel can not only fulfil superficial enamel reconstruction, but also effectively suppress bacterial infection and subsequent demineralization.

4. Conclusions

In summary, taking advantage of the potential of amelogenin to control the organized growth of apatite crystals and the potential antimicrobial activity of chitosan we have developed a new amelogenin-containing chitosan hydrogel for superficial enamel reconstruction. Amelogenin assemblies stabilized Ca-P clusters in a CS-AMEL hydrogel and guided their arrangement into linear chains. These amelogenin–Ca-P composite chains further fused with enamel crystal and eventually evolved into enamel-like co-aligned crystals, anchored to the natural enamel substrate through a cluster growth process [47,48]. The continuous growth of crystals formed an excellent bond between the newly grown layer and the enamel. Furthermore, the hardness and elastic modulus of etched enamel were increased by nine and four times after treatment with CS-AMEL hydrogel. We anticipate that this chitosan hydrogel will provide effective protection against secondary caries because of its pH-responsive and antimicrobial properties. Our studies introduce a promising CS-AMEL hydrogel method for superficial enamel repair and demonstrate the potential of applying protein-directed assembly to the biomimetic reconstruction of complex biomaterials.

Acknowledgements

This research was supported by NIH-NIDCR grants DE-13414 and DE-020099 to J.M.O. The authors would like to thank Dr Sisi Liu for assistance with the transmission electron microscopy, and the Center for Electron Microscopy and Microanalysis (CEMMA) at USC for electron microscopy.

Appendix A. Figures with essential colour discrimination

Certain figures in this article, particularly Figures 1, 3–6 and 8, are difficult to interpret in black and white. The full colour images can be found in the on-line version, at http://dx.doi.org/10.1016/j.actbio.2013.04.004.

References

[1] Moradian-Oldak J. Protein-mediated enamel mineralization. Front Biosci 2012;17:1996–2023.
[2] Cui FZ, Ge J. New observations of the hierarchical structure of human enamel, from nanoscale to microscale. J Tissue Eng Regen Med 2007;1:185–91.
[3] Fincham AG, Moradian-Oldak J, Simmer JP. The structural biology of the developing dental enamel matrix. J Struct Biol 1999;126:270–99.
[4] Bartlett JD, Simmer JP. Proteinases in developing dental enamel. Crit Rev Oral Biol Med 1999;10:425–41.
[5] Ruttermann S, Trellenkamp T, Bergmann N, Raab WHM, Ritter H, Janda R. A new approach to influence contact angle and surface free energy of resin-based dental restorative materials. Acta Biomater 2011;7:1160–5.
[6] Onuma K, Yamagishi K, Oyane A. Nucleation and growth of hydroxyapatite nanocrystals for nondestructive repair of early caries lesions. J Cryst Growth 2005;282:199–207.
[7] Busch S. Regeneration of human tooth enamel. Angew Chem Int Ed 2004;43:1428–31.
[8] Guentsch A, Busch S, Seidler K, Kraft U, Nietzsche S, Preshaw PM, et al. Biomimetic mineralization: effects on human enamel in vivo. Adv Eng Mater 2010;12B:571–6.
[9] Yamagishi K, Onuma K, Suzuki T, Okada F, Tagami J, Otsuki M, et al. A synthetic enamel for rapid tooth repair. Nature 2005;433:819.
[10] Chen H, Tang Z, Liu J, Sun K, Chang S-R, Peters MC, et al. Acellular synthesis of a human enamel-like microstructure. Adv Mater 2006;18:1846–51.
[11] Li L, Mao C, Wang J, Xu X, Pan H, Deng Y, et al. Bio-inspired enamel repair via glu-directed assembly of apatite nanoparticles: an approach to biomaterials with optimal characteristics. Adv Mater 2011;23:4695–701.
[12] Yin YJ, Yun S, Fang JS, Chen HF. Chemical regeneration of human tooth enamel under near-physiological conditions. Chem Commun 2009:5892–4.
[13] Li L, Pan HH, Tao JH, Xu XR, Mao CY, Gu XH, et al. Repair of enamel by using hydroxyapatite nanoparticles as the building blocks. J Mater Chem 2008;18:4079–84.
[14] Xie RQ, Feng ZD, Li SW, Xu BB. EDTA-assisted self-assembly of fluoride-substituted hydroxyapatite coating on enamel substrate. Cryst Growth Des 2011;11:5206–14.
[15] Qi YP, Li N, Niu LN, Primus GM, Liang JQ, Pashley DH, et al. Remineralization of artificial dentinal caries lesions by biomimetically modified mineral trioxide aggregate. Acta Biomater 2012;8:836–42.
[16] Fletcher J, Walsh D, Fowler CE, Mann S. Electrospun mats of PVP/ACP nanofibres for remineralization of enamel tooth surfaces. Crystengcomm 2011;13:3692–7.
[17] Petta V, Moradian-Oldak J, Yannopoulos SN, Bouropoulos N. Dynamic light scattering study of an amelogenin gel-like matrix in vitro. Eur J Oral Sci 2006;114:308–14.
[18] Iijima M, Moradian-Oldak J. Control of apatite crystal growth in a fluoride containing amelogenin-rich matrix. Biomaterials 2005;26:1595–603.
[19] Iijima M, Du C, Abbott C, Doi Y, Moradian-Oldak J. Control of apatite crystal growth by the co-operative effect of a recombinant porcine amelogenin and fluoride. Eur J Oral Sci 2006;114:304–7.
[20] Du C, Falini G, Fermani S, Abbott C, Moradian-Oldak J. Supramolecular assembly of amelogenin nanospheres into birefringent microribbons. Science 2005;307:1450–4 [Erratum, Science 2005;309:2166].
[21] Fan Y, Sun Z, Moradian-Oldak J. Controlled remineralization of enamel in the presence of amelogenin and fluoride. Biomaterials 2009;30:478–83.
[22] Fan Y, Sun Z, Wang R, Abbott C, Moradian-Oldak J. Enamel inspired nanocomposite fabrication through amelogenin supramolecular assembly. Biomaterials 2007;28:3034–42.
[23] Wang L, Guan X, Yin H, Moradian-Oldak J, Nancollas GH. Mimicking the self-organized microstructure of tooth enamel. J Phys Chem C 2008;112:5892–9.
[24] Lee H-S, Tsai S, Kuo C-C, Bassani AW, Pepe-Mooney B, Miksa D, et al. Chitosan adsorption on hydroxyapatite and its role in preventing acid erosion. J Colloid Interface Sci 2012;385:235–43.
[25] Stamford Arnaud TM, Barros Neto B, Diniz FB. Chitosan effect on dental enamel de-remineralization: an in vitro evaluation. J Dent 2010;38:848–52.

[26] Decker EM, von Ohle C, Weiger R, Wiech I, Brecx M. A synergistic chlorhexidine/chitosan combination for improved antiplaque strategies. J Periodontal Res 2005;40:373–7.
[27] Rabea EI, Badawy MET, Stevens CV, Smagghe G, Steurbaut W. Chitosan as antimicrobial agent: applications and mode of action. Biomacromolecules 2003;4:1457–65.
[28] Neilands J, Sutherland D, Resin A, Wejse PL, de Paz LEC. Chitosan nanoparticles affect the acid tolerance response in adhered cells of *Streptococcus mutans*. Caries Res 2011;45:501–5.
[29] de Paz LEC, Resin A, Howard KA, Sutherland DS, Wejse PL. Antimicrobial effect of chitosan nanoparticles on Streptococcus mutans biofilms. Appl Environ Microbiol 2011;77:3892–5.
[30] Dash M, Chiellini F, Ottenbrite RM, Chiellini E. Chitosan – a versatile semi-synthetic polymer in biomedical applications. Prog Polym Sci 2011;36:981–1014.
[31] Henson BS, Wong DT. Collection, storage, and processing of saliva samples for downstream molecular applications. In: Seymour GJ, Cullinan MP, Heng NCK, editors. Oral biology: molecular techniques and applications. Totowa, NJ: Humana Press; 2010. p. 21–30.
[32] Selwitz RH, Ismail AI, Pitts NB. Dental caries. Lancet 2007;369:51–9.
[33] Cheng ZJ, Wang XM, Cui FZ, Ge J, Yan JX. The enamel softening and loss during early erosion studied by AFM, SEM and nanoindentation. Biomed Mater 2009;4:1–7.
[34] Murugan R, Ramakrishna S. Aqueous mediated synthesis of bioresorbable nanocrystalline hydroxyapatite. J Crys Growth 2005;274:209–13.
[35] Li B, Wang Y, Jia D, Zhou Y. Gradient structural bone-like apatite induced by chitosan hydrogel via ion assembly. J Biomater Sci Polym Ed 2011;22:505–17.
[36] Lakshminarayanan R, Fan D, Du C, Moradian-Oldak J. The role of secondary structure in the entropically driven amelogenin self-assembly. Biophys J 2007;93:3664–74 [Erratum, Biophys J 2008;94:715].
[37] Fan DM, Iijima M, Bromley KM, Yang XD, Mathew S, Moradian-Oldak J. The cooperation of enamelin and amelogenin in controlling octacalcium phosphate crystal morphology. Cells Tissues Organs 2011;194:194–8.
[38] Fan D, Du C, Sun Z, Lakshminarayanan R, Moradian-Oldak J. In vitro study on the interaction between the 32 kDa enamelin and amelogenin. J Struct Biol 2009;166:88–94.
[39] Liu WG, Sun SJ, Cao ZQ, Xin Z, Yao KD, Lu WW, et al. An investigation on the physicochemical properties of chitosan/DNA polyelectrolyte complexes. Biomaterials 2005;26:2705–11.
[40] Edgar WM. Role of saliva in control of pH changes in human dental plaque. Caries Res 1976;10:241–54.
[41] Stephan RM. PH and dental caries. J Dent Res 1947;26:340.
[42] Lingstrom P, van Ruyven FOJ, van Houte J, Kent R. The pH of dental plaque in its relation to early enamel caries and dental plaque flora in humans. J Dent Res 2000;79:770–7.
[43] Onuma K, Ito A. Cluster growth model for hydroxyapatite. Chem Mat 1998;10:3346–51.
[44] Posner AS, Betts F. Synthetic amorphous calcium-phosphate and its relation to bone-mineral structure. Acc Chem Res 1975;8:273–81.
[45] Fang PA, Conway JF, Margolis HC, Simmer JP, Beniash E. Hierarchical self-assembly of amelogenin and the regulation of biomineralization at the nanoscale. Proc Natl Acad Sci USA 2011;108:14097–102.
[46] Yang X, Wang L, Qin Y, Sun Z, Henneman ZJ, Moradian-Oldak J, et al. How amelogenin orchestrates the organization of hierarchical elongated microstructures of apatite. J Phys Chem B 2010;114:2293–300.
[47] Pouget EM, Bomans PHH, Goos J, Frederik PM, de With G, Sommerdijk N. The initial stages of template-controlled $CaCO_3$ formation revealed by cryo-TEM. Science 2009;323:1455–8.
[48] Gebauer D, Volkel A, Colfen H. Stable prenucleation calcium carbonate clusters. Science 2008;322:1819–22.
[49] Mehdawi I, Neel EA, Valappil SP, Palmer G, Salih V, Pratten J, et al. Development of remineralizing, antibacterial dental materials. Acta Biomater 2009;5:2525–39.
[50] Cuy JL, Mann AB, Livi KJ, Teaford MF, Weihs TP. Nanoindentation mapping of the mechanical properties of human molar tooth enamel. Arch Oral Biol 2002;47:281–91.
[51] Eimar H, Ghadimi E, Marelli B, Vali H, Nazhat SN, Amin WM, et al. Regulation of enamel hardness by its crystallographic dimensions. Acta Biomater 2012;8:3400–10.
[52] Yang XD, Sun Z, Ma RW, Fan DM, Moradian-Oldak J. Amelogenin "nanorods" formation during proteolysis by Mmp-20. J Struct Biol 2011;176:220–8.
[53] Sun Z, Carpiaux W, Fan D, Fan Y, Lakshminarayanan R, Moradian-Oldak J. Apatite reduces amelogenin proteolysis by MMP-20 and KLK4 in vitro. J Dent Res 2010;89:344–8.
[54] Gorgieva S, Kokol V. Preparation, characterization, and in vitro enzymatic degradation of chitosan–gelatine hydrogel scaffolds as potential biomaterials. J Biomed Mater Res A 2012;100A:1655–67.
[55] Liu XF, Guan YL, Yang DZ, Li Z, De Yao K. Antibacterial action of chitosan and carboxymethylated chitosan. J Appl Polym Sci 2001;79:1324–35.